APPLICATION OF TOPSIS IN DISTRIBUTION SYSTEM MULTI-OBJECTIVE OPTIMIZATION

Andrea MAZZA, Gianfranco CHICCO

Politecnico di Torino, Energy Department, Torino, Italy

REZUMAT. Această lucrare prezintă o aplicație al algoritmului de decizie TOPSIS pentru a obține soluții nedominate prin optimizarea multiobiectiv a unui sistem de distribuție de medie tensiune rezolvat prin metoda NSGA-II. Obiectivele considerate se bazează pe economia de energie (pierderile totale) şi pe un indicator de fiabilitate (energia totală nefurnizată). Ambele obiective sunt subiectul minimizării. Sunt prezentate detalii privind determinarea indicatorului de fiabilitate. Rezultatele arată ordonarea soluțiilor nedominate pentru un studiu de caz bazat pe o rețea de testare clasică.

Cuvinte cheie: sisteme de distribuție, optimizare, multi-obiectiv, pierderi, fiabilitate, TOPSIS.

ABSTRACT. This paper presents an application of the TOPSIS decision-making tool to rank the non-dominated solutions originated by the multi-objective optimization of a Medium Voltage distribution system solved through the NSGA-II method. The objectives considered are based on energy saving (total losses) and on a reliability indicator (total energy not supplied). Both objectives are subject to minimization. Details on the determination of the reliability indicator are provided. The reported results show the ranking of the non-dominated solutions for a case study based on a classical test network.

Keywords: distribution system, optimization, multi-objective, losses, reliability, TOPSIS.

1. INTRODUCTION

In the present evolution of the electricity distribution systems, many aspects are being subject to upgrade and modernization, both on the components side (smart metering and distribution automation) and on the formulation of the calculation methods (with new tools for distribution system optimization in operation and planning contexts)[1][2]. The objective functions for optimization are evolving from the classical ones (total losses, investment&operation costs, load balancing) to a more extended set of objectives taking into account voltage and reactive power support, reliability and environmental impact.

Optimization by using different objectives may lead to highly different results. In particular, the objectives may be conflicting with each other, that is, the best solutions for one objective could correspond to relatively worse solutions for the other objectives. In the presence of conflicting objectives, the key concept is the one of *non-dominated* solutions. These solutions are the ones for which it is not possible to find any other solution having all better objectives. The rationale for multi-objective optimization is to find the set of non-dominated solutions, called *Pareto front* [3].

Multi-objective solutions have been addressed in distribution system optimization by using deterministic or heuristic methods to find out the non-dominated solutions located in the pseudo-optimal approximation of the Pareto front [4]–[7]. The optimization problem can be formulated by resorting to a discrete number of combinations to be analyzed, as in the case of distribution system optimization. However, the distribution network sizes generally prevent from carrying out an extensive calculation of all the possible combinations. The use of heuristic methods that can drive the solutions towards the true Pareto front is then of particular interest. An example of heuristic method solving the Pareto front calculation efficiently is NSGA-II (Non-dominated Sort Genetic Algorithm) [8]. The use of NSGA-II as a general-purpose tool (included in the Matlab® Global Optimization Toolbox) requires particular care in the handling of the equality and inequality constraints.

The Pareto front resulting from the optimization tool provides a number of solution points, that have to be compared with each other in order to decide which solution is the most viable to be implemented. The decision-maker could privilege his/her own solution based on personal judgement, but in many cases a post-processing stage is needed for the purpose of sending to the decision-maker a priority message among the solutions obtained. This post-processing stage is generally absent in the papers concerning distribution system multi-objective optimization.

This paper calculates the multi-objective optimization solutions for a distribution system through the application of NSGA-II and proposes the application of a specific tool such as TOPSIS [9] to perform post-processing of the solutions obtained. The objectives considered are the total losses and the energy not supplied. Both objectives have to be minimized. A detailed view is provided on the implementation of the reliability calculations.

The remainder of this paper is organized as follows. Section 2 deals with recalling the distribution system structures and with introducing the objective functions and constraints. Section 3 describes the reliability implementation concepts. Section 4 recalls the usage of TOPSIS for ranking the Pareto front solutions. Section 5 presents the results of a case study application. The last section contains the concluding remarks.

2. MULTI-OBJECTIVE DISTRIBUTION SYSTEM OPTIMIZATION

Distribution system structure.

The electricity distribution system has one or more supply points and a *weakly meshed structure*, but it is operated under *radial configurations* by opening the redundant branches, such that simple protection schemes can be exploited. If the distribution system has more than one supply point at the MV side (for instance, *S* supply points), in the radial operation there are *S* radial networks, each of which is supplied by one supply point.

For each radial network, it is possible to identify the *root* (or *slack*) *node*, corresponding to the supply point of the radial network and taken at the MV side of the HV/MV transformer. The slack node forms the supply layer, here called layer 0. From the MV busbars of the HV/MV substation, there are in general multiple *feeders* connecting the slack node to a subset of nodes. Let us consider this subset of nodes as the nodes forming the layer 1. Let us then consider the subset of nodes connected to the nodes belonging to layer 1, identified as nodes belonging to layer 2. By proceeding with the same rationale, the nodes belonging to layer 2 are connected to (other) nodes forming the layer 3, and so forth until all the nodes have been allocated to a layer. Clearly, if the network is radial all the nodes can be allocated to a layer by construction. Conversely, if the network is not radial two situations may occur:

1) at least one node has already been allocated to a previous layer and is attempted to be located to a successive layer during the construction process;
2) at the end of the node allocation to the layers, there are one or more nodes that have not been visited during the construction process.

The sending terminal of the branches connecting the slack node to the other nodes contains the protection devices (e.g., the circuit breakers). The branches connected to the nodes of the layers beyond layer 1 contain only switching devices, and no circuit breaker. It is then easy to note that a fault occurring on a branch implies the trip of the circuit breaker located in the supply substation and the subsequent lack of the supply of all the nodes belonging to the radial network to which this branch is connected. In order to restore the system operation after a (permanent[1]) fault, the location of the faulted branch has to be identified (e.g., through a trial-and-error process). Then, the set of nodes that remain isolated after the fault has to be identified as well, the faulted branch has to be open and the supply has to be restored to the isolated nodes. This process depends on the nature of the system nodes and on the fault search strategy used (Section 3).

Objective functions and constraints.

Since the distribution system has a weakly meshed structure, it is necessary to form the radial networks supplied by each supply point by identifying the redundant branches to keep open. For this purpose, it is possible to formulate an objective function, such that the set of open branches will result from its minimization or maximization. More generally, it is possible to set up a multi-objective optimization of the distribution system operation, as the one addressed in this paper considering two optimization objectives:

1) the total network losses;
2) the total energy not supplied (*ENS*), as defined in Section 3.

These objectives are conflicting with each other, as there is no direct correlation between distribution network losses and reliability. To confirm the conflicting nature of these objectives, the solution of the multi-objective problem will provide a Pareto front with a number of possible compromise solutions (while in the absence of conflicting solutions the Pareto front would collapse into a single point).

The other constraints refer to the thermal limits of the branches, and the upper and lower node voltage limits. The branch-exchange mechanism [10] is applied

[1] The distinction among temporary and permanent faults is illustrated in Section 3.

to preserve the network radiality when the use of genetic operators could lead to non-radial solutions.

The main constraint of the problem is the network radiality. The constraints are implemented by discarding any solution leading to violation of one or more constraint.

3. DESCRIPTION OF THE RELIABILITY ASPECTS

Representation of the distribution network nodes and types of fault.

The nodes of the distribution network can be of two main types:

- *Automated nodes*: the branches connected to these nodes contain switches that are controlled by the distribution system operator acting from the control centre.
- *Manually-controlled nodes*: the branches connected to these nodes contain switches that have to be operated locally by a maintenance team.

The operation on an automated node is quicker (on the average) than an operation on a manually-controlled one. The different durations of connection of an isolated portion of the network after a permanent fault are reported in Table 1. It is worth to remark that the duration of the circuit breaker operation is not considered in the computation of the reliability indicator, being much smaller than the other durations.

The redundant branches resulting from a radial configuration are kept open, but typically only one of the switches located at one terminal is open, while the other one remains closed to make the on/off switching operations easier. In general, the side with the lower automation degree is closed (linked to the network), while the terminal with the higher automation degree is switchable to permit quick reconfiguration. In case the two terminals have the same degree of automation, the choice of the branch to keep open is either arbitrary, or can be the subject of a sub-optimization procedure.

It is important to discern between *temporary* and *permanent* faults. In the first case, the fault is self-cleared and causes a service interruption of relatively short duration. The restoration of the supply occurs at the first automatic reclosure of the circuit breaker located in the branch connected to the slack node and supplying the portion of the network containing the faulted branch.

For permanent faults, if a closed branch is faulted, the loads connected by this branch to the supply side remain unserved. This is a problem both for the customers and for the distribution system operator: the customers are not supplied, while the distribution system operator increments its unreliability indicators and could be subject to penalties if the relevant indicator (e.g., energy not supplied) exceeds the limits imposed by the regulatory authority in a given observation period (e.g., one year).

Table 1

Duration of connection of an isolated portion of the network to an alternate supply using a redundant branch

open branch with	duration of connection to another feeder [h]
both automated terminals	0.05
both manually-controlled terminals	1
at least one automated terminal	0.05
absence of alternate supply point (fault repair awaited)	15

The fault search has been implemented in different ways, in according to the automation degree of the switching, the state of the branch (redundant or operative) and the localization of the fault.

In general, the supply restoration contains different steps. The first step is the fault search in which, thanks to the operations on the automated and the manual switches, together with the circuit breaker of the relevant feeder, the faulted or damaged branch is found and open. After that, the supply of the node placed upstream the faulted branch can be restored. Then, it is necessary to find all alternative paths linking the downstream nodes with respect to the faulted branch, and restore their supply.

It is important to note that, in the procedure presented above, both the presence of double supply points and the possibility of two consecutive faults (i.e., a second fault occurring before the first fault has been repaired and the service has been restored) are neglected. These hypotheses are in line with the ones typically used in the analytical methods for distribution system reliability [11].

Energy not supplied.

The reliability indicator used in this paper is the Energy Not Supplied (*ENS*) [12]–[15]. The formulation of the reliability calculations follows the multi-stage reliability model illustrated in [16]. In particular, let us consider the rated load power C_k of node $k = 1,...,N$, and the time interval of observation $[0,T]$. The detection of the fault f, in general, can be composed of H_f different stages. During the h-th stage, node k can be either supplied or not supplied, and this information is stored in the binary variable $b_{fk}^{(h)}$, which is equal to unity if the

k-th node is not supplied during the h-th search stage of the fault f, and zero otherwise. Then, it is possible to obtain the value of the total power not supplied during the h-th search stage of the fault f:

$$P_f^{(h)} = \sum_{k=1}^{N} C_k \cdot b_{fk}^{(h)} \qquad (1)$$

Furthermore, let $\boldsymbol{\theta}_k$ be the set containing all the faults which imply that the node k is not supplied and $\tau_f^{(h)}$ the expected value of the duration of the h-th restoration procedure. The expected value of the energy not supplied at node k is computed as:

$$ENS_k = C_k \cdot \sum_{f \in \boldsymbol{\Theta}_k} \sum_{h=1}^{H_f} \lambda_f \cdot b_{fk}^{(h)} \cdot \tau_f^{(h)} \qquad (2)$$

where λ_f is the fault rate of the fault f.

In general, the fault search has been implemented in this way:

- fault search using the automated switches, and identification of the portion of the network containing the faulted branch and located between two successive automated switches;
- fault search using the manual switches to find the fault location and to isolate the faulted branch from the rest of the network;
- supply of the loads located both upstream and downstream with respect to the faulted branch, closing where possible the redundant branches to energize the nodes located downstream with respect to the faulted branch.

Computation of the interruption duration.

The computation of the interruption duration is done after the calculation of the number of manual and automatic switching. Knowing the number of nodes of the network N (slack excluded), it is possible to create the vector of manual actions $\mathbf{n}_{MM}$ and the vector of automated ones $\mathbf{n}_{AM}$. Both vectors have dimensions Nx1. Their k-th element represents the number of either manual or automated actions of the k-th node. Some elements of these vectors are equal to zero, because a node can be only either with manual or automated switching.

Then, it is necessary to consider the time needed to energize the isolated part of the network. So, another vector $\mathbf{r}_T$ is introduced, with dimensions Nx1, whose elements either represent the restoration time (if an alternate supply point is absent) or the time to connect the portion of network to another feeder.

By knowing $\mathbf{n}_{MMf}$, $\mathbf{n}_{AMf}$, and $\mathbf{r}_{Tf}$ (respectively, the number of manual and automated switchings, and the restoration time corresponding to the fault f), and considering the fault rate λ_f, the automated switch time of action τ_{AS} and the manual switch time of action τ_{MS}, it is possible to compute the vector $\boldsymbol{\tau}_f$ (dimensions Nx1), which contains the time for which the nodes are not supplied due to the fault f:

$$\boldsymbol{\tau}_f = \lambda_f \cdot [\tau_{AS} \cdot \mathbf{n}_{AMf} + \tau_{MS} \cdot \mathbf{n}_{MMf} + \mathbf{r}_{Tf}] \qquad (3)$$

Finally, introducing the set $\boldsymbol{\Theta}$ containing all possible faults and the vector $\mathbf{c}$ containing the nominal bus loads of each node, the ENS is given by:

$$ENS = \mathbf{c}^{\mathrm{T}} \cdot \sum_{f \in \boldsymbol{\Theta}} \boldsymbol{\tau}_f \qquad (4)$$

Identification of the alternate supply paths.

In a multi-feeder network (that is, with more branches connecting the slack node to the nodes belonging to layer 1) the presence of an alternate supply is given by the existence of a branch connecting the non-energized part of the network to another feeder.

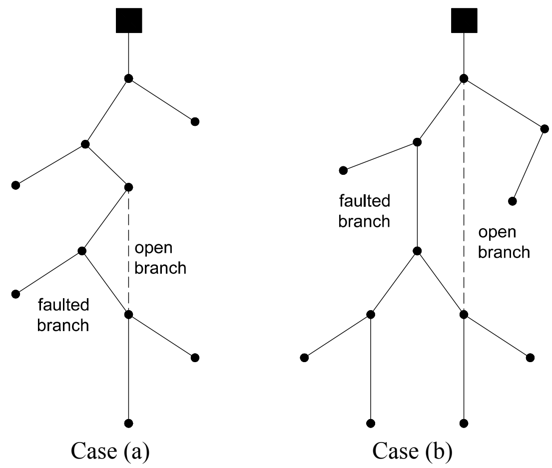

Fig. 1. Two examples of network with only one feeder. The black-filled square boxes represent the HV/MV sub-stations.

If only one feeder is present (that is, only one branch connects the rest of the network with the slack node), an alternate supply could still exist. In fact, let us refer to Fig. 1, where two networks with only one feeder are presented, and let us consider two cases in which the alternate supply for all nodes energized by the faulted branch is guaranteed:

- Case (a): a redundant branch connects the downstream node and a node placed upstream with respect to the fault.
- Case (b): the open branch connects a node energized by the fault and a node that supplies the faulted branch and belongs to a different subfeeder, not containing the fault (the figure shows the extreme case in which the upstream node is both belonging to the subfeeder containing the faulted branch and to another subfeeder).

The implementation of the fault search strategy has some differences in the cases of fault on a closed branch or fault on an open branch (considering the side at which the branch is connected to the network). Full simulation of the operations to locate the fault is implemented in order to calculate the *ENS* indicator.

4. RANKING THE PARETO FRONT SOLUTIONS WITH TOPSIS

Generalities on TOPSIS.

TOPSIS [9] is a ranking method which permits the re-ordering of a number of alternatives following the opinion of the decision maker.

First of all, it is necessary to choose the *weights* of the evaluation criteria (also called objectives): since they form completely the objective space, the sum of their weights has to be equal to unity.

TOPSIS is based on the knowledge of the *decision matrix* **A**. If N_A is the number of the alternatives and N_C is the number of the criteria, the dimension of the matrix **A** will be N_A xN_C.

The decision matrix **A** is obtained using the eigenvalue Saaty's method [17]: it is based on the computation of N_C pair comparison matrices $\mathbf{D}_j$, with j=1,....,N_C. These matrices tell us how much a certain solution is better than the other solutions, considering each evaluation criterion, one at a time. The evaluation is done using the Saaty's scale, which is composed of nine levels (from 1 to 9): for instance, if a certain solution p is low better than a solution k (considering the i-th evaluation criterion), the corresponding element d^i_{pk} will be equal to 2. Conversely, if the element p is low worse than a solution k (considering the j-th evaluation criterion), the corresponding element d^j_{pk} will be equal to ½. Since that, all the pair comparison matrices are symmetrical.

The Saaty's scale is reported in Table 2.

The principal eigenvalue μ_j of each matrix $\mathbf{D}_j$ and its corresponding eigenvector $\mathbf{u}_j$ are found. Then, the normalized eigenvectors $\mathbf{u}^*_j$ are computed: in fact, each eigenvector is defined up to a constant and the constant is placed such that the sum of the eigenvector's components is equal to unity. The decision matrix has as columns these normalized eigenvectors.

Then, the elements r_{ij} belonging to the normalized decision matrix **R** are computed from the elements a_{ij} of the decision matrix **A** in the following way:

$$r_{ij} = \frac{a_{ij}}{\sqrt{\sum_{k=1}^{N_A} a_{kj}^2}} \tag{5}$$

with j=1,....,N_C and i=1,...,N_A. It is important to note that this normalization is necessary because in the matrix **A** different measurement units can be present.

Table 2

Values of the number of generations by changing the crossover fraction

d^i_{pk}	**Explanation**
1	The solutions p and k are equally important
3	The solution p is slightly more important than the solution k
5	The solution p is much more important than the solution k
7	The solution p is strongly more important than the solution k
9	The solution p is absolutely more important than the solution k
2,4,6,8	Intermediate levels

After that, the weighted normalized decision **V** is obtained as a matrix with the following component:

$$v_{ij} = r_{ij} \cdot w_j \tag{6}$$

with w_j representing the weight of the j-th criterion.

At this point, the positive ideal solution A^+ and the negative ideal solution A^- are computed: the first one represents the ideal point of **V** having the best value in each objective; the A^- represents the point of **V** having the worst value of the objectives for each criterion. If the two objectives are costs, then A^+ will have the lowest value at each criterion; instead, if the two objectives are benefits, A^+ will have the highest value at each criterion. Then, the Euclidean distances from A^+ and A^- and each solution are calculated:

$$ED_i^+ = \sqrt{\sum_{j=1}^{N_C} (v_{ij} - v_j^+)^2} \tag{7}$$

$$ED_i^- = \sqrt{\sum_{j=1}^{N_C} (v_{ij} - v_j^-)^2} \tag{8}$$

with i=1,...,N_A. Thanks to these distances, it is possible to compute the normalized distance from the negative ideal solution A^-:

$$ED_{i,rel}^- = \frac{ED_i^-}{ED_i^- + ED_i^+} \tag{9}$$

By using this value for each alternative, the ranking of all the alternatives is possible. For instance, it is possible to use this method for ranking the solutions composing the Pareto front.

TOPSIS implementation for ranking the pseudo-optimal solutions.

In this paper, a modified version of the crossover fucntion of [18] is used. It is characterized by the *local improvement* which permits the further improvement of the objectives with respect to the configuration obtaining by the simple crossover.

In the original article [18], the authors start by mixing the genes belonging to the *main parent* and to the *secondary parent*: using a random point of cutting, the genes belonging to the main parent and placed between the first one and that one indicating by the point of cutting, are copied in the offspring. After that, the chromosome is filled using the elements of the secondary parent not present yet, and such that they do not form any loop. Starting from this configuration, the loops obtained closing one at time the redundant branches are found. So, the alternative configurations obtained by exchanging one open branch and one of the closed branches forming the loop are analysed: in the original article, when a *better* solution is found, the algorithm passes to another open branch, repeating the same routine.

In this paper, all the alternative solutions obtained by each loop (in other words, from each redundant branch) are analysed. From them, the pseudo-optimal solution is chosen. In a multi-objective problem, it is necessary to rank in some way the solutions, to choose the best one. In a mono-objective optimization (as in the original article), the choice is simple because it is possible to choose (in case of a minimization problem) the solution having the *minimum* value of the objective. With two or more objectives, it is necessary to apply a ranking method in which the different evaluation criteria can be considered.

In this paper, the TOPSIS methods has been applied in the choice of the best solution from the Pareto front obtained. TOPSIS is also applied to the choice of the pseudo-optimal solution among the configuration obtained by each application of the branch-exchange mechanism (the number of branch-exchange applications at each stage of the solution process is equal to the number of open branches).

5. CASE STUDY APPLICATION

Network structure and data.

The test network used is the classical IEEE 14-node network (Fig. 2). The network has three supply points, conceptually merged into a single slack node called node 0.

The rated (nominal) values are A_N=100 MVA and V_N=23 kV. The branch impedances and the nodal loads are reported in the Appendix.

Determination of the Pareto front.

First of all, using a deterministic method, all the solutions of the networks have been computed (Fig. 3a); after that, the three solutions composing the full Pareto front are obtained (Fig. 3b), using the concept of non-dominance in the Pareto sense. The non-dominated solutions are reported in Table 3. Applying the TOPSIS method to the values reported in Table 3, the ranked solutions are the ones shown in Table 4.

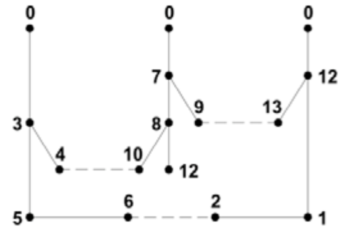

Fig. 2. The IEEE 14-node test network.

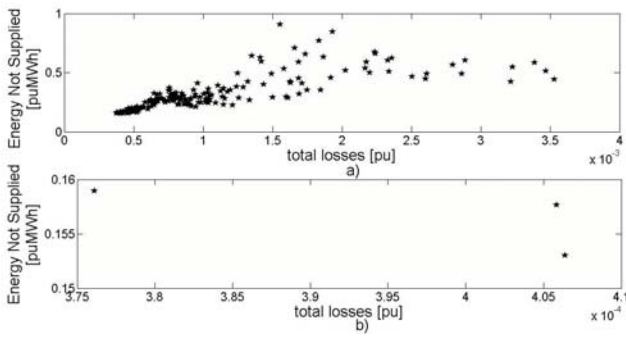

Fig. 3. a) the 190 configurations of the test network; b) the complete Pareto front.

Table 3

Values of the non-dominated solutions of the network

total losses [pu]	*ENS* [pu_{MWh}]
0.00037611	0.158933
0.00040638	0.153033
0.00040583	0.157635

Table 4

Values of the non-dominated solutions of the network

rank	total losses [pu]	*ENS* [pu_{MWh}]
1	0.00040638	0.153033
2	0.00037611	0.158933
3	0.00040583	0.157635

After the ranking of the solutions, the first test is made. The input data are the following:

- probability of mutation: p_m = 0.8;
- crossover fraction: c_f= 0.6;
- initial population: 4 individuals;
- weights: 0.5 for each objective;

• tolerance for the stop criterion: 10^{-8};

• maximum number of successive generations for which the improvement of the average spread of the multi-objective solutions is lower than the tolerance: 70 (stop criterion, as implemented in the Matlab® Global Optimization Toolbox).

In the case shown, the customized genetic algorithm has found only 2 solutions at the 8th iteration (Fig. 4): it is interesting to remark that the two solutions found are the two more important ones following the ranking of Table 4.

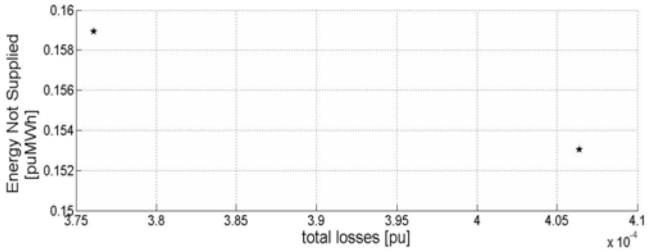

Fig. 4. Pareto front obtained in the first test.

Then, only the size of population is changed and set equal to 5 individuals: the customized genetic algorithm finds all solutions belonging to the Pareto front at the 11th iteration.

Now, maintaining both the probability of mutation and the crossover fraction constant, the weights are changed; the number of generations in which the complete Pareto front is obtained is reported in Table 5.

Table 5

Values of the number of generations by changing the weights

losses weigth	number of generations
0.1	24
0.2	33
0.3	15
0.4	15
0.5	11
0.6	10
0.7	10
0.8	10
0.9	29

Then, using the same value of p_m, and placing the losses weight equal to 0.5, the c_f is changed: the step is 0.2 because of the size of the population. In fact, to obtain almost one configuration by the mutation routine, it is necessary to set c_f=0.8, while to obtain almost one configuration by the crossover routine it is necessary to set c_f=0.2. The number of iterations (generations) in which the algorithm finds the complete Pareto front is reported in Table 6.

Table 6

Values of the number of generations by changing the crossover fraction

c_f	0.2	0.4	0.6	0.8
number of generations	9	6	11	17

Then, by setting c_f equal to 0.4 and maintaining the losses weight equal to 0.5, the p_m is changed. The number of generations in which the algorithm finds all solutions belonging to the Pareto front is reported in Table 7.

Table 7

Values of the number of generations by changing the crossover fraction

p_m	0.1	0.2	0.3	0.4	0.5	0.6	0.7	0.8	0.9	1
generations	11	5	5	13	10	26	6	6	12	8

6. CONCLUSIONS

The current developments of distribution system optimizations are highlighting the importance of taking into account multiple objectives, in many cases with conflicting nature. The solutions provided by multi-objective optimization belonging to a Pareto front represent compromise solutions, and each of these solutions may be of practical interest. The NSGA-II tool has been used to find directly the solutions belonging to the Pareto front by starting from an initial set of solution points and upgrading the Pareto front iteratively. In the case study application shown in this paper, all the non-dominated solutions have been found, as confirmed by running exhaustive search on all configurations.

A ranking criterion has been applied to the multi-objective solutions to assist the decision-makers in undertaking their decisions. The TOPSIS method has been used for ranking the solutions forming the Pareto front. A case has been shown in which not all the Pareto front solutions have been found, finding out anyway the two top-ranked solutions. Other results have been reported by changing the weights of the TOPSIS objectives and the probabilities of crossover and mutation within NSGA-II, indicating that no regularity appears in the convergence of NSGA-II to find out the complete Pareto front for the test system analyzed.

APPENDIX

Table A1

Rated power of the loads and local generation systems used in the IEEE 14-node network. The negative signs represent the generation units

node	rated *P* [kW]				
	residential	industrial	tertiary	photovoltaic	hydro
1	100	100	150	0	0
2	100	100	150	0	0
3	100	100	150	0	0
4	100	100	150	0	0
5	100	100	150	-20	0
6	100	100	150	0	-150
7	100	100	120	0	0
8	100	100	120	0	0
9	100	150	120	0	0
10	100	100	100	0	0
11	100	100	120	0	0
12	100	100	100	0	0
13	100	100	150	0	0

Table A2

Values of tgφ used for the different types of load

type of load or generation	tgφ
residential	0.1
industrial	0.5
tertiary	0.4
photovoltaic	0
hydro	0

Table A3

Branch impedances for the IEEE 14-node system

branch	R [pu]	X [pu]	branch	R [pu]	X [pu]
0 – 3	0.075	0.1	9 – 13	0.04	0.04
3 – 4	0.08	0.11	12 – 13	0.09	0.12
4 – 10	0.04	0.04	0 – 12	0.11	0.11
8 – 10	0.11	0.11	1 – 12	0.08	0.11
8 – 11	0.08	0.11	1 – 2	0.04	0.04
7 – 8	0.08	0.11	2 – 6	0.09	0.12
0 – 7	0.11	0.11	5 – 6	0.04	0.04
7 – 9	0.11	0.11	3 – 5	0.09	0.18

BIBLIOGRAPHY

[1] **Fan J., Borlase S.**, *The evolution of distribution*, IEEE Power & Energy Magazine, Vol. 7, No. 2, 2009, pp. 63–68.

[2] **Chicco G**., *Challenges for Smart Distribution Systems: Data Representation and Optimization Objectives*, 12th International Conference on optimization of electrical and electronic equipment (OPTIM 2010), Brasov, Romania, 20-22 May 2010, pp. 1236–1244.

[3] **Shukla P.K., Deb K.**, *On finding multiple Pareto-optimal solutions using classical and evolutionary generating methods*, European Journal of Operational Research, Vol. 181, 2007, pp. 1630–1652.

[4] **Roytelman I., Melnik V., Lee S.S.H., Lugtu R.L.**, *Multiobjective feeder reconfiguration by distribution management system*, IEEE Trans. on Power Systems, Vol. 11, No. 2, 1996, pp. 661–667.

[5] **Hsiao Y.-T., Chien C.-Y.**, *Multiobjective optimal feeder reconfiguration*, IEE Proc. C, Gener. Transm. Distrib., Vol. 148, 2001, pp. 330–336.

[6] **Das D.**, *A fuzzy multiobjective approach for network reconfiguration of distribution systems*, IEEE Trans. on Power Delivery, Vol. 21, No. 1, 2006, pp. 202–209.

[7] **Mendoza J.E., Lopez M.E., Coello C.A.C., Lopez E.A.**, *Microgenetic multiobjective reconfiguration algorithm considering power losses and reliability indices for medium voltage distribution network*, IET Generation, Transmission & Distribution, Vol. 3, No. 9, 2009, pp. 825–840.

[8] **Deb K., Pratap A., Agarwal S., Meyarivan T.**, *A fast and elitist multiobjective genetic algorithm: NSGA-II*, IEEE Trans. on Evolutionary Computation 6 (2), April 2002, pp. 182–197.

[9] **Hwang, C.L., Yoon, K**., *Multiple attribute decision making. Methods and applications: a state-of-the-art survey.* Berlin and New York: Springer-Verlag, 1981.

[10] **Civanlar S., Grainger J., Yin H., Lee S.**, *Distribution feeder reconfiguration for loss reduction*, IEEE Trans. on Power Delivery, Vol. 3, No. 3, 1988, pp. 1217–1223.

[11] **Carpaneto, E., Chicco, G.**, *Evaluation of the probability density functions of distribution system reliability indices with a characteristic functions-based approach*, IEEE Trans. on Power Systems, Vol.19, No.2, 2004, pp.724–734.

[12] **Billinton R., Allan R.N.**, *Reliability Evaluation of Power Systems*, New York: Plenum Press, 1984.

[13] **Billinton R.**, *Distribution System Reliability Performance and Evaluation*, Electrical Power & Energy Systems, Vol. 10, No. 3, 1998, pp. 190–200.

[14] **Brown R.E.**, *Reliability of distribution systems*, New York: Dekker, 2002.

[15] **Endrenyi J.**, *Reliability Modeling in Electric Power Systems*, New York : Wiley & Sons, 1978.

[16] **Carpaneto, E., Chicco, G.**, *Analytical reliability evaluation of large urban distribution systems with multi-phase load restoration*, International Journal of Engineering Intelligent Systems for Electrical Engineering & Communications, Vol. 11, No. 4, 2003, pp.209–216.

[17] **Saaty, T.L.**, *A scaling method for priorities in hierarchical structures*, Journal of Mathematical Psychology, 1977, pp. 234–281.

[18] **Carreno, E. M., Romero, R., Padilha-Feltrin, A.**, *An efficient codification to solve distribution network reconfiguration for loss reduction problem*, IEEE Trans. on Power Delivery, Vol. 23, No. 4, 2008, pp. 1542–1550.

About the authors

Dr. Eng. **Andrea MAZZA**
Politecnico di Torino, Energy Department, corso Duca degli Abruzzi 24, 10129 Torino, Italy.
email:andrea.mazza@polito.it

Graduated at Politecnico di Torino (PdT), Torino, Italy, in 2011. He is currently a Ph.D. student in Electrical Engineering at PdT. His research activities include power system and distribution system analysis and optimization, and multi-criteria decision-making. He is a member of the Italian Federation of Electrical, Electronic and Telecommunications Engineers (AEIT).

Prof. Eng. **Gianfranco CHICCO**, PhD
Politecnico di Torino, Energy Department, corso Duca degli Abruzzi 24, 10129 Torino, Italy.
email:gianfranco.chicco@polito.it

Graduated at Politecnico di Torino (PdT), Torino, Italy, received the Ph.D. degree in Electrotechnical Engineering from PdT in 1992. Currently, he is a Professor of Electrical Energy Systems at PdT. His research activities include power system and distribution system analysis, load management, energy efficiency, artificial intelligence applications, and power quality. He is a Senior Member of the IEEE and a member of the Italian Federation of Electrical, Electronic and Telecommunications Engineers (AEIT).